Singh and Singh
*Micro and Nano Systems Letters* (2023) 11:20
https://doi.org/10.1186/s40486-023-00182-x

Micro and Nano Systems Letters

LETTER

Open Access

# Dispersion and agglomeration of carbon nanoclusters in 4-(trans-4′-hexylcyclohexyl)-isothiocyanatobenzene media on ITO and graphene surfaces: role of surface effect

Archana Kumari Singh[1] and Satya Pal Singh[1*]

**Abstract**

We have synthesized carbon nanoparticles using mandarin juice via green synthesis rout. We have doped carbon nanoparticles in liquid crystal media and studied the surface effect on self-assembly of carbon nanoclusters on ITO coated glass surface and on graphene sheet. The purpose of this study is to construct uniform nano-micro droplets for novel applications and to understand and explore the underlying science behind molecular scale reorganization in the presence of functional surfaces like graphene. We have used density functional theory approach to confirm that the carbon nanoparticles in globular structures are dispersed in presence of graphene sheet due to chemical interaction of carbon rings (or say carbon nanoparticles) with graphene carbon atoms. In order to minimize the free energy, the carbon nanoparticles leave the carbon globular structures and are dispersed to form rectangular structures in presence of LC media at graphene surface. The carbon nanoparticles are dispersed to increase contact area with graphene surface. The results are useful in construction of desired nano-micro structures for possible novel purposes in medical field since carbon nanoparticles are biocompatible. Optical microscopy, FESEM, NMR and UV spectra verifies the droplet formation and its effect on the surface and electronic properties of carbon nanoparticles.

**Keywords** Density functional theory, Mandarin juice, Single layer graphene sheet, ITO, FESEM, NMR

## Introduction

Nanotechnology has made amazing progress, resulting in the development of novel functional materials and their nanostructures with applications in a wide range of fields. One such new area of research is the production and characterization of nano-micro droplets, which have unique features due to their size and biocompatibility [1]. Recently, nano colloidal particle-containing liquid crystal (LC) suspensions have attracted significant interest for a variety of practical applications, including nano sensors. Liquid crystal display [2], optical processing, biosensors [3], photonics [4], and magneto-optics etc. [5]. New materials with unique properties are required for the new applications, as well as for making new technologies. For instance, adaptive LC optics requires LC materials with enormous birefringence and low viscosity, while LC materials for telecommunications typically call for LCs with strong birefringence but low refractive index. Particle introduction results in a reduction in driving voltages, an increase in reaction contrast, and a steeper transition.

Natural carbon-based nanoparticles are extremely rare, and the vast majority of them are either engineered or artificially synthesized. As a result, their availability is not dependent on natural reserves (such as diamonds), and production can theoretically be performed in infinite quantities as long as raw materials

*Correspondence:
Satya Pal Singh
singh.satyapal@hotmail.com
[1] Department of Physics and Material Science, Madan Mohan Malaviya University of Technology, Gorakhpur, UP 273010, India

for synthesis are available. According to the most recent projections, production volumes will continue to rise over the next decade. Despite the fact that carbon-based nanomaterials promote industrial progress, there are concerns about the potential environmental release, interactions of released nanomaterials with living organisms, and their incorporation into food chains, all of which have yet to be determined and understood quantitatively [6, 7]. Carbon is one among the few chemical elements which has the capacity to polymerize at the atomic level forming very long carbon chains, along with silicon. Carbon atoms have a valency of four due to the presence of four electrons in the outer most shell and it can be joined by single, double, or triple covalent bonds. Carbon atoms may exist in sp, $sp^2$ and $sp^3$ hybridization states. Not only that in highly curved nanoparticles like carbon nanotubes and buckyballs, some of hybridized states of the type $sp^n$, where n is a fraction between 1–2 and 2–3. Carbon atoms unique electronic structure and smaller size in comparison to other group IV elements can be used to explain these characteristics. For the reasons outlined above, carbon can exist in a variety of different molecular forms that are all made of the same type of atoms (i.e. carbon allotropes) but differ in their structures and properties. Because of the reasons, the geometrical structures of carbon-based nanomaterials are used to categorize them most frequently [8, 9].

Graphene has attracted considerable interest in a variety of fields due to its $\pi$-rich electronic structure, two-dimensional (2D) layered structure, and ease of functionalization, as well as because of its excellent mechanical, thermal, optical, and electrical properties [10]. In practical applications, graphene interact dynamically with small molecules, particles, or ions near its surface, which is critical in many physical and chemical processes. In this paper, we have investigated the interactions between graphene sheets and carbon nanoclusters in order to better understand the functional properties of graphene surface. The graphene surface has two types of interactions: covalent and non-covalent. Covalent interactions are most common in chemisorbed molecules/atoms, resulting in relatively small distance separations (2.0 Å − 3.0 Å) and strong orbital overlapping with graphene. In general, the covalent interaction force appears in the covalent functionalization reaction of graphene. It is an intramolecular force with a strong interaction. This interaction is primarily present in organic molecules, free radicals, and graphene C=C bonds or oxygen-containing groups. In general, covalent functionalization reactions necessitate specific reaction conditions. The dynamic interactions on the graphene surface are mostly due to weak interactions (non-covalent) causing physio-sorption and are characterized by a distance value ranging between 3.0 Å and 5.0 Å [11].

Graphene is chemically inert from the perspective of highly crystalline, pristine graphene. However, in theory, environmental media can interact with the surface of graphene through non-covalent bonds like ion-$\pi$ interactions, van der Waals interactions, $\pi$-$\pi$ interactions, and hydrophobic interactions due to the electronic structure of the large pi-bond and its 2D layered structure. The $\pi$-$\pi$ interaction is a specific type of supramolecular force. It primarily refers to the interaction between two aromatic rings in a restricted sense. Graphene's hydrophilicity changes as functional groups are added to it. van der Waals force is the net result of the attraction and repulsion forces that occurs between atoms or molecules as a result of the correlation of the wave polarization of adjacent particles. Three forces orientation force, inductive force, and dispersion forces are primarily responsible for it. For graphene surfaces, it is one of the prominent interactions. The atomic configuration of the graphene plane and, consequently, the physical properties of graphene are generally not much affected by the van der Waals's force. Large $\pi$ bonds provide weak interactions between graphene layers and atoms or molecules of other materials. It may also assist in graphene's electronic conduction. When it comes to metals, the type of metal substrate and particular manufacturing procedure typically affect the bonding forces with the graphene surface [12–14].

Droplet microfluidics has the potential for higher throughput and scalability than continuous flow systems. Several groups have used droplet microfluidics in the last five years to create irregular particles, double emulsions, hollow microcapsules, and microbubbles. These particles have a wide range of applications, including biomolecule synthesis, drug delivery, and diagnostic testing [15–21]. Due to low-cost raw materials and environment friendly production techniques, the production of carbon nanomaterials from bio-precursors is of utmost importance. Papaya peel scraps were used to hydrothermally create carbon quantum dots (CQDs) without any surface passivation [22]. Researchers have drawn attention to the interaction between CQDs and the E7 liquid crystal [23]. In LC mesophase, a strong coupling of CQDs is seen [24]. Electro-optical characterization of CQDs made from oil palm leaves in E48 LC at various doping concentrations has been performed previously [25]. The impact of graphene on various particles has been previously investigated to explore its potential applications. Different types of microstructures have been synthesized using CQDs [26]. Jing Zhan et al. conducted a thorough evaluation of studies on the interactions of graphene with various things such as molecules, particles, and ions. The

surface contact with graphene affects the behaviour and properties of molecules/particles/ions due to interaction with graphene [27]. Seung-Rak Son et al. reported surface-anchored alkylated graphene oxide (AGO) to achieve homeotropic alignment of nematic liquid crystals (NLCs). To provide amphiphilic properties, amino reactions with dodecyl amine are used to functionalize the GO. The hydrophobic alkyl chains of AGO govern the preferred direction of the NLCs [28] as they create a 2D-alignment layer on the indium tin oxide surface via polar affinity. A graphene-based composite with an internal three-dimensional (3D) conductive network was used by Xin Meng et al. to create a highly electrical and thermal conductive film. Between the layers of graphene oxide (GO), the cellulose nanocrystalline (CNC) phase with chiral liquid crystal appears in the three-dimensional (3D) framework aligned to helix. Carbon nanodots (CDs) are used inside the nanocomposites as conductive nanofillers [29]. Recent developments using the above processes have been summarized by Zhimin Chai et al. They also discuss how these directed self-assembly processes harness the external fields. They have highlighted the underlying mechanism of how the external fields interact with the nanoelements, and the benefits and drawbacks of using each technique [30]. G. M. Alcantar et al. have investigated the phenomenon, contributing to the advances in the understanding of the processes involved to design new sensing platforms based on AIECL [31]. We have studied the surface effect of graphene on self-assembly of ZnO and MgO nanoparticles in 6CHBT LC media on ITO coated and plane glass surfaces [32]. The self-assembly of silver nanoparticles and nano-micro clusters formation has also been observed and reported by us [33].

While our prior research work was focused to the other features of carbon nanodots and liquid crystals self-assembly, a full knowledge of the synergistic effects in the context of nano-micro droplets in presence of graphene and ITO coated glass is still lacking. The properties of nano-micro droplets composed of carbon nanodots in presence of LC media on ITO and graphene coated surfaces have been investigated in depth in this paper, highlighting their optical absorption, and photoluminescence, properties as well as exploring their surface properties in a comparative manner. The incorporation of various substrates, such as indium tin oxide (ITO) and graphene sheets, adds another layer of intricacy to the investigation. These substrates are critical in altering the characteristics of the nano-micro droplets, expanding their potential uses in optoelectronic devices. ITO is a transparent conductive material with high electrical conductivity and optical transparency. It is widely used in optoelectronic applications such as screens, sensors, and solar cells. ITO was used as a substrate due to its compatibility with liquid crystal and carbon nanodots. The interaction between ITO and nano-micro droplets can affect the charge transport and optical properties. By studying the behaviour of nano-micro droplets on ITO, we hope to gain a better understanding of the substrate's possible impact on their optoelectronic properties and investigate their applicability for transparent and conductive device applications. Graphene a single sheet of hexagonally organized carbon atoms has remarkable electrical, thermal, and mechanical properties. Because of its large surface area and distinct electrical properties, it is a good candidate for a variety of electronic and optoelectronic applications. We wish to take advantage of the molecular interaction between graphene and nano-micro droplets composed of carbon nanoparticles. The electronic characteristics of graphene can influence charge transport and energy transfer processes within droplets, potentially resulting in improved optoelectronic functions. This

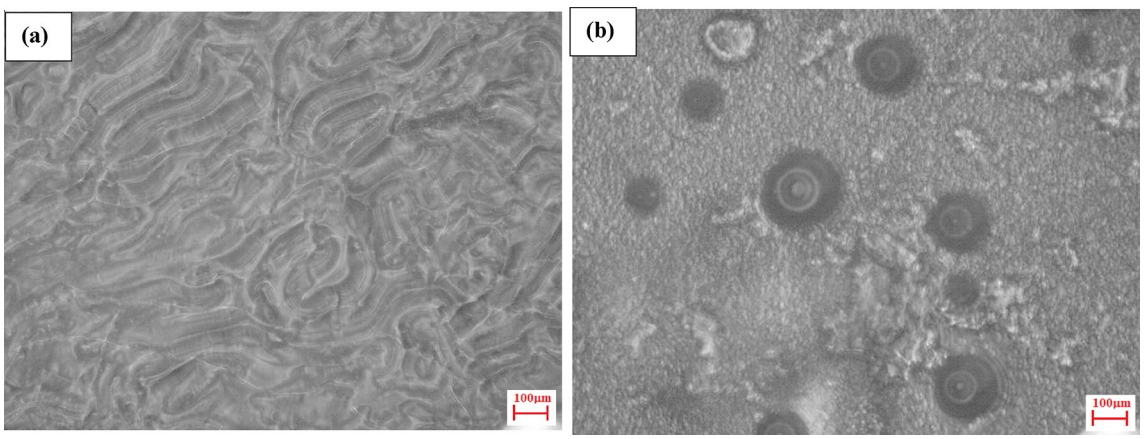


**Fig. 1** Optical Microscopy images of the different part of the samples on ITO coated glass surface

novel substrate provides a new dimension to our inquiry, allowing us to investigate the interaction between carbon nanodot-based nano-micro droplets and graphene sheet having extraordinary properties.

## Methodology

### Material required

Mandarin juice, 4-(trans-4-n-hexylcyclohexyl) isothiocyanatobenzoate (6CHBT) liquid crystal purchased from Sigma Aldrich (99% pure), has been used with no further purification required. Throughout the experiment, we used de-ionized water. Among the other items, we need ethanol, 60 μm Mylar strips used as spacers, acetone, and so on. In order to conduct the experiment, only analytical research grade chemicals were used.

### Synthesis of carbon nanoparticles

To synthesize carbon nanoparticles in less time, a green, cost-effective microwave assisted strategy is widely used. As a carbon source, mandarin juice was chosen. Carbon nanoparticles synthesized from mandarin juice have unique features that make them attractive for a variety of applications. When exposed to UV or visible light, they glow strongly, making them useful for imaging and sensing applications. Because of their biocompatibility, they can be used in biological and medicinal purposes. Their tunable features allow for customization to fit specific needs. Furthermore, carbon nanoparticles synthesized with mandarin juice provide an environmentally benign and sustainable way to nanomaterial fabrication. These features, combined with low toxicity and the ability to surface functionalize, expand their utility in a variety of domains, including bio-imaging, drug delivery, and catalysis etc. [34, 35]. The first stage in the synthesis is to create an emulsion in which carbon nanoparticles are produced from mandarin juice in dispersed phase. The temperature at the time of emulsification is critical in determining droplet size and stability. Because of the increased kinetic energy, higher temperatures frequently result in smaller droplets, with larger interfacial area. Longer processing times at controlled temperatures produce more consistent emulsions because they allow carbon nanoparticles to be completely incorporated into the emulsion mixture. Variations in mandarin juice concentration can also change the number density of the carbon nanoparticles accessible for integration, affecting the overall droplet composition.The mandarin was purchased locally and washed with tap water. 50 ml mandarin juice was subsequently extracted by hand. It was transferred to a beaker and heated in an oven at 60 °C for 24 h. After that, place the solution in a crucible and heat it with steam for 24 h at 120 °C. The obtained

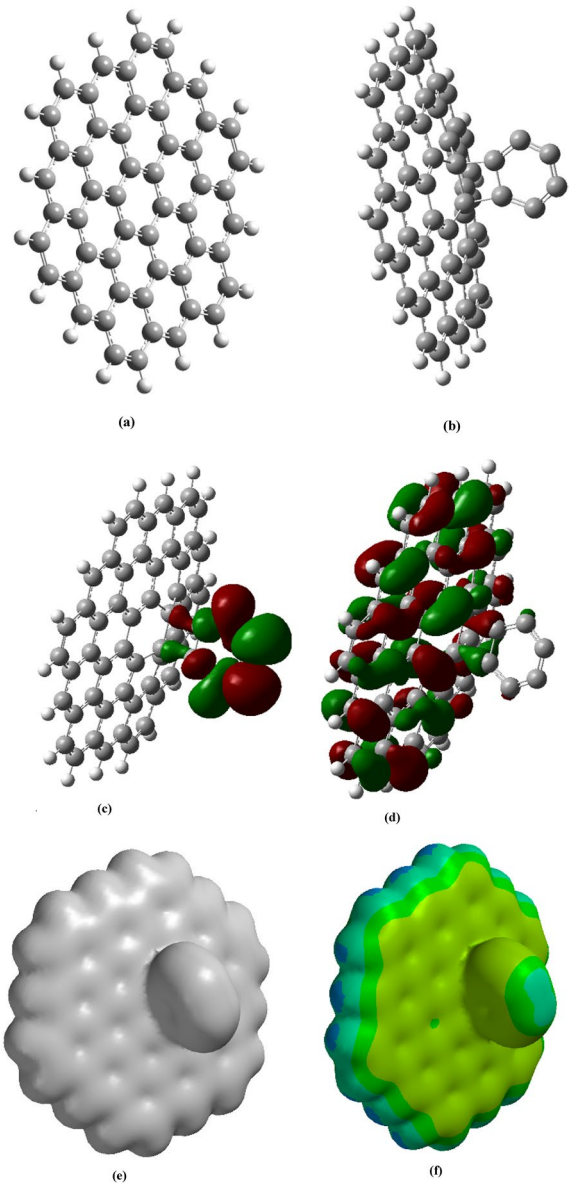


**Fig. 2** Optimized structures of **a** graphene sheet, **b** six carbon atoms cluster linked graphene surface **c** LUMO orbital picture of graphene and carbon ring **d** HOMO orbital picture of graphene and carbon ring **e** electron density surface and **f** electrostatic potential surface map of the optimized carbon cluster on graphene surface. **a**-**d** to are obtained using DFT calculations via Gaussian software and **e**–**f** are obtained using DFT calculations via Spartan 20 software

brown-black solution mixture was filtered and centrifuged for 1 h at 4,000 rpm. The supernatant was kept at 4 °C for future experiments and characterization.

The homogeneous and isotropic mixture of liquid crystals and nanoparticles was created by dissolving the two components in toluene. The solvent is then slowly evaporated by vacuum drying. To create

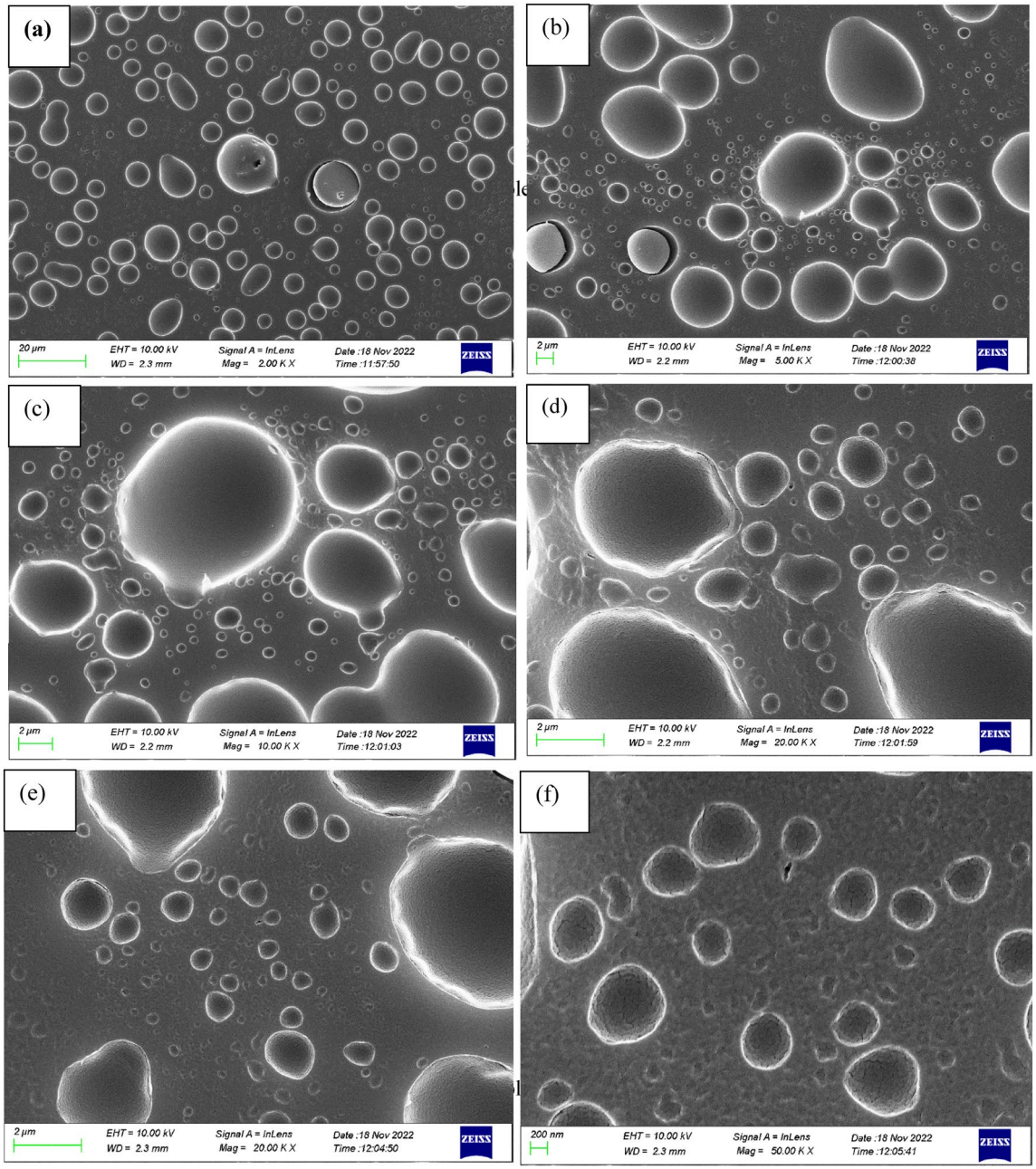


**Fig. 3** FESEM images of the different part of samples in different resolutions on ITO coated glass surface

a homogeneous solution, we bath sonicated 0.5 mg carbon nanoparticles NPs, 102 µL 6CHBT LC in 5 ml toluene solution for 3 h at 50 °C. We obtained a clear solution and placed it in a 60 °C oven to evaporate the remaining toluene. 60-m thick cells were formed by sandwiching Mylar strips (spacers) between a substrate and a cover. Again, we prepare the same cell for graphene surface by placing graphene sheet on glass substrate, then Mylar strips, and finally glass cover.

## Results and discussion

### Optical microscopy

Optical Microscope images were obtained using inverted optical microscope (Zeiss) of 0.1 resolution and objestive lens of 100 × oil immersion/1.25 and 20x/0.30. Optical microscopy is used to analyze the overall morphology and size distribution of the synthesized nano-micro droplets. This technique allow us to evaluate the macroscopic aspects of the droplets and to determine their

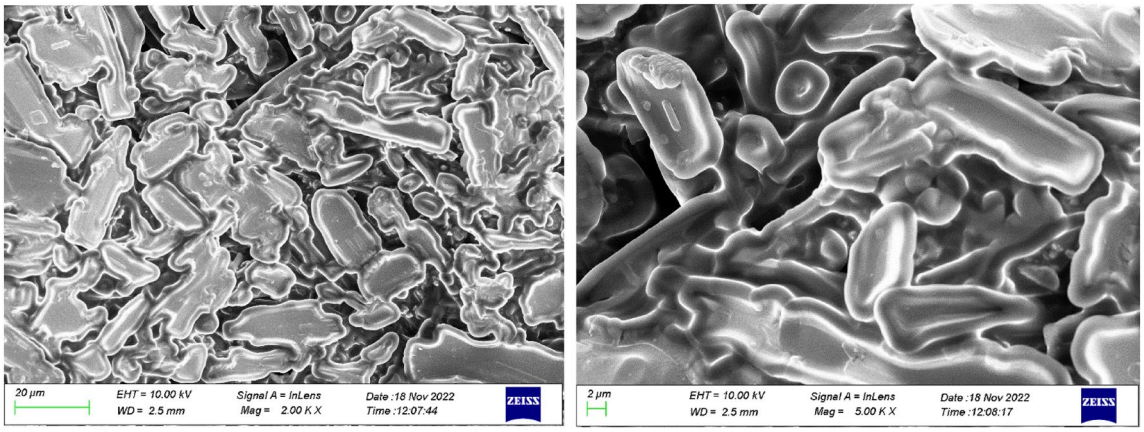


**Fig. 4** FESEM images of the different part of samples in different resolutions on graphene surface

homogeneity. It helps to acquire first insights into their structural characteristics. Optical microscopy images show the agglomeration of carbon nanomaterials and anchoring of LC molecules over its surface.

Figure 1 shows the optical microscopy images of carbon nanomaterials doped LC system on ITO coated glass surface. Figure 1a, b show the micron sized droplet formation. Due to the strong intermolecular interactions among carbon nanoparticles than intramolecular interactions between carbon and ITO molecules, show agglomeration and form dense droplets at the surface Spherical droplets (globular structures) are formed under conditions of low external influence, when surface tension predominates by carefully managing parameters such as temperature, pressure, and surface characteristics. The surface of the aggregated carbon nano-micro clusters flattens and produces flattened nano-micro structures in presence of graphene substrate because of the molecular interaction between the carbon nanoparticle and the graphene. We have performed a quantum simulation using density functional method using B3LYP basis set [36]. We have first obtained optimized structure of graphene-like molecule by placing hydrogen atoms at terminal carbon atoms because of the practical reason as infinitely extended graphene sheet will require extra ordinary huge computational power. To test the type of interaction, we restrict our study to a carbon ring formed by placing six carbon atoms placed on the vertex of a hexagon and have again simulated to obtain the final hybridized composite structures as shown in Fig. 2a, b using Gaussian software. A hexagonal ring structure made of six carbon atoms first appears in form of ring inclined parallel to the surface of graphene like plane. In latter phase of the optimization process the ring composed of carbon atoms becomes perpendicular to the graphene surface. The unhybridized p orbitals of carbon atoms are aligned perpendicular to the graphene sheet and overlap side wise to form $\pi$-bonds. This orbital can also interact with the orbital of foreign carbon atoms, reducing energy and forming stabilized structures as observed in Fig. 2a, b.The orbital overlapping is observed for *LUMO* orbitals in Fig. 2c and *HOMO* orbitals in Fig. 2d. The overlapping of orbitals confirms the strong interaction between the carbon atoms in carbon nanoparticles and graphene surface. This could be possible and accounted only on the basis delocalization of electrons via $\pi$-bonds.Atoms and molecules are made up of positively charged nuclei surrounded by a negatively charged electron cloud. The size and form of an atom or molecule are defined by the electron cloud rather than the nuclear skeleton. The electron density (the number of electrons per unit volume) describes their distribution as well as size and form of an atom. The electron density surface of the globally stabilized carbon cluster on graphene sheet is shown in Fig. 2e obtained using Spartan 20 software. An electron density surface that maps the electrostatic potential value is depicted in Fig. 2f. The surface itself correlates to the electron density and provides a measure of the molecule's overall size and shape. The colors represent electrostatic potential values on this surface. Colors towards red are associated with negative potential (a stable association between the molecule and a positive charge), while colors towards blue are associated with positive potential.

### FESEM images

FESEM data have been obtained using SUPRA 40 VP (Zeiss) apparatus. FESEM is used to examine the nano-micro droplet structures in more detail. We are able to investigate the surface morphology, particle configurations, and probable nanoparticle aggregation within the droplets using this technique, which produces high-resolution images.The surface morphologies of carbon

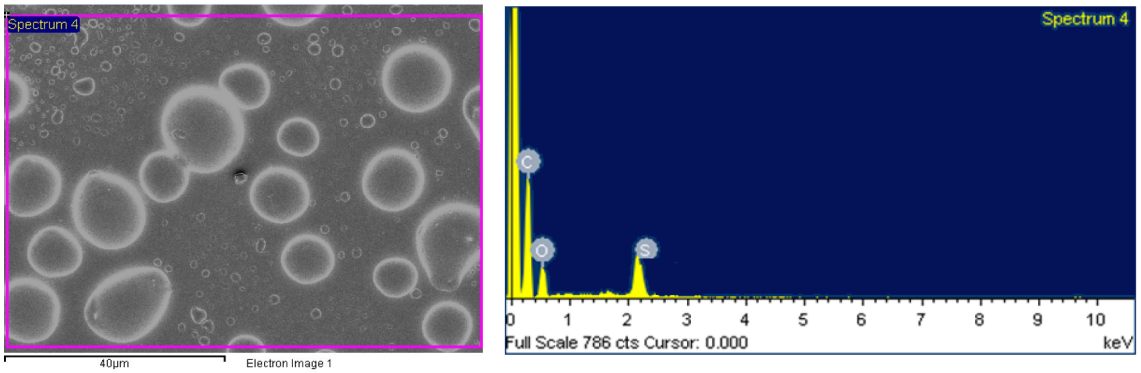


| Element | Weight% | Atomic% |
|---|---|---|
| C K | 60.93 | 67.34 |
| O K | 39.08 | 32.61 |
| S L | 0.35 | 0.04 |
| Totals | 100.00 | |

**Fig. 5** EDX spectrum of Carbon nano-micro cluster formation in LC media on ITO coated glass surface

nanocluster doped 6CHBT LC system on ITO coated glass surface and on single layer graphene sheet can be observed clearly by FESEM images. Figure 3 shows different part of the samples in different resolutions. Carbon nanoclusters agglomerates and from nano-microdroplets on the ITO glass surface. Dense droplets formation are observed on this surface because of lower intramolecular interactions as shown in Fig. 3a, b. Figure 3c,d, e and f show the carbon nanoclusters agglomerates and forms orange-like nano-micro droplets (or shells). Some of the droplets colesce to each other anf forms bigger droplet. Further in higher magnification as presented in Fig. 3e, nanodroplets are configured having cell like surface morphology. Due to $\pi$-$\pi$ ineteractions present in graphene sheet, this affects the intermolecular force among carbon nanoparticles and thus, the shape of the spherical droplets transformed to flat droplets as presented in Fig. 4. Figure 4a, b shows the droplets collesce together and due to strong intramolecular interactions forms some ractangular flat random structures. Some of carbon nanoclusters assemble in blood cells like morphology in this case as observed in Fig. 4b.

In the case of ITO-coated glass, the ITO layer is commonly composed of indium oxide ($In_2O_3$) and tin oxide ($SnO_2$). Carbon atoms in various forms (such as carbon nanotubes or graphene) can interact with the ITO surface via weak van der Waals forces only. As a result, carbon nanoparticles prefer to self-assemble, forming nano-micro spheres or globular structures on an ITO-coated glass surface to reduce surface energy. Carbon nanoparticles, on the other hand, are effectively attracted by the graphene surface due to chemisorption reaction and do not form nano-micro globular structure as in case of graphene. Covalent interactions are primarily seen in chemisorbed molecules/atoms, resulting in relatively close separation of nearly 2–3 A˚ as observed due to strong orbital overlaps with graphene. It is an intramolecular force with high degree of contact.

### EDX analysis

EDX analysis is used to identify the chemical components of nanomaterials. The elemental makeup of the nanomaterial is determined by detecting and studying the characteristic X-rays produced when the sample is hit with an electron beam. EDX also provide semi-quantitative or quantitative statistics on the relative abundance of different components. The hybrid system's Energy Dispersive X-ray (EDX) characterization was carried out utilizing an Argon vacuum created inside the FESEM-EDX [SUPRA 40 VP (Zeiss)]. To perform the analysis, a thin gold film coating is first applied to the surface of the sample. The material is imaged qualitatively and quantitatively using EDX. The existence of carbon atoms in the LC sample is confirmed by the EDX spectrum. The elemental weight

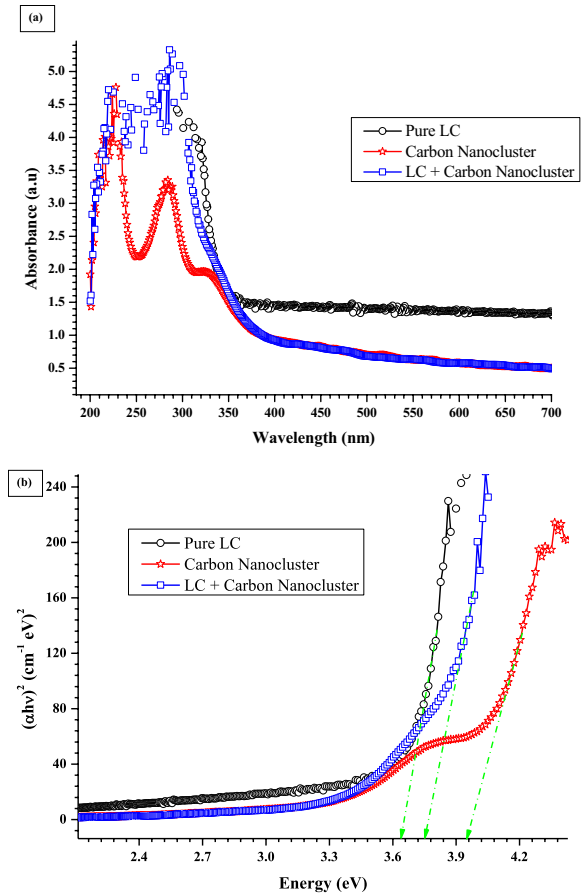


**Fig. 6** **a** UV–vis spectra and **b** Tauc plots of pure LC, carbon nanocluster, and carbon nanocluster doped LC media

percentages of C (60.93 wt%) and S (0.35 wt%) in the 6CHBT LC molecule (C19H27NS) are shown. The entire spectrum is located in energy bands corresponding to K lines ranging from 0.2 to 3.5 keV. The highest wt percent of carbon implies the production of carbon dots in LC media on an ITO- coated glass surface. The system's EDX spectrum is depicted in Fig. 5. The peak corresponding to N is missing here. It is challenging to record the presence of all the species present in the sample instantly using EDX. Presence of very small traces of impurity atoms may also be recorded on some occasions.

## UV-vis–nir spectroscopy

UV–vis-nir spectra for carbon nanoclusters, pure LC and its combinations are observed using Shimadazu UV -visible 1900i. UV–vis-nir spectroscopy is used to investigate the optical characteristics of the synthesised materials. We are able to identify the UV, visible, and near-infrared absorption and transmission properties of nano-micro droplets using UV–vis-nir spectroscopy. The UV–vis-nir observation was taken in solution form, and solution was made in ethanol. In order to measure the absorbance of carbon nanoclusters, UV–visible spectrophotometer is used to record UV–visible spectra in the absorbance mode in the wavelength range 200–700 nm as shown in Fig. 6a. The absorption peaks are obtained in the range 200 nm to 350 nm. Broad peak in this range (i.e., near 250 nm) shows the synthesized nanoparticles possess quantum confinement. To determine the energy band gap of carbon nanocluster, pure LC, and carbon nanocluster doped LC system, Tauc's relation was employed.

$$(\alpha h\nu) = A(h\nu - E_g)^n \tag{1}$$

Here n is a constant which is equal to 1/2 for the direct band gap, h is the Planck's constant, A is a constant, $E_g$ is the energy band gap, and $\alpha$ is the absorption coefficient. Extrapolating the curve drawn between $(h\nu)$ and$(\alpha h\nu)^2$, the band gaps of the Pure LC, Carbon nanocluster, and carbon nanoclusters with LC were calculated from Fig. 6b. The optical absorption coefficient is indicated by the symbol $\alpha$, where $\nu$ indicates the frequency. The energy band gap was observed by extrapolating the curve with the help of tangent line, were found to be 3.64 eV, 3.95 eV, and 3.75 eV for pure LC, carbon nanocluster, and carbon nanocluster doped LC system, respectively. After nano-micro droplet formation the bandgap of the system shifts to the value 3.75 eV.

We have employed a theoretical model to further elucidate the creation of nano/micro clusters. The relationship between the bandgap of NPs and their bulk counterpart is described by Eq. (1), for reference for this model one can check all discussions from our research paper [33].

Thus,

$$E_g(n) = E_g(Bulk)\left(1 + \frac{n_s}{n}\right) \tag{2}$$

Here, $E_g(Bulk)$ is the bandgap for the bulk case, $E_g$ (n) is the bandgap for the nanoparticles case. $n_s$ is the number of atoms present at the surface of NPs.n is total number of atoms present. We extended this idea to the case of carbon NP clusters. We assume four possible shapes of carbon nanoclusters in presence of liquid crystal molecules as spherical, tetrahedral, hexahedral, and octahedral shapes and find out the best one which perfectly matches with our experimental data. From Tauc's plot the bandgap of synthesized carbon nanodots is 3.95 eV. The bandgap value of carbon in bulk case is 3.30 eV [37]. Using the prominent peak observed in the UV–vis data of carbon nanoclusters we have calculated the approximate size of the synthesized carbon nanocluster is found to be 40.297 nm. Remember this carbon nanocluster is

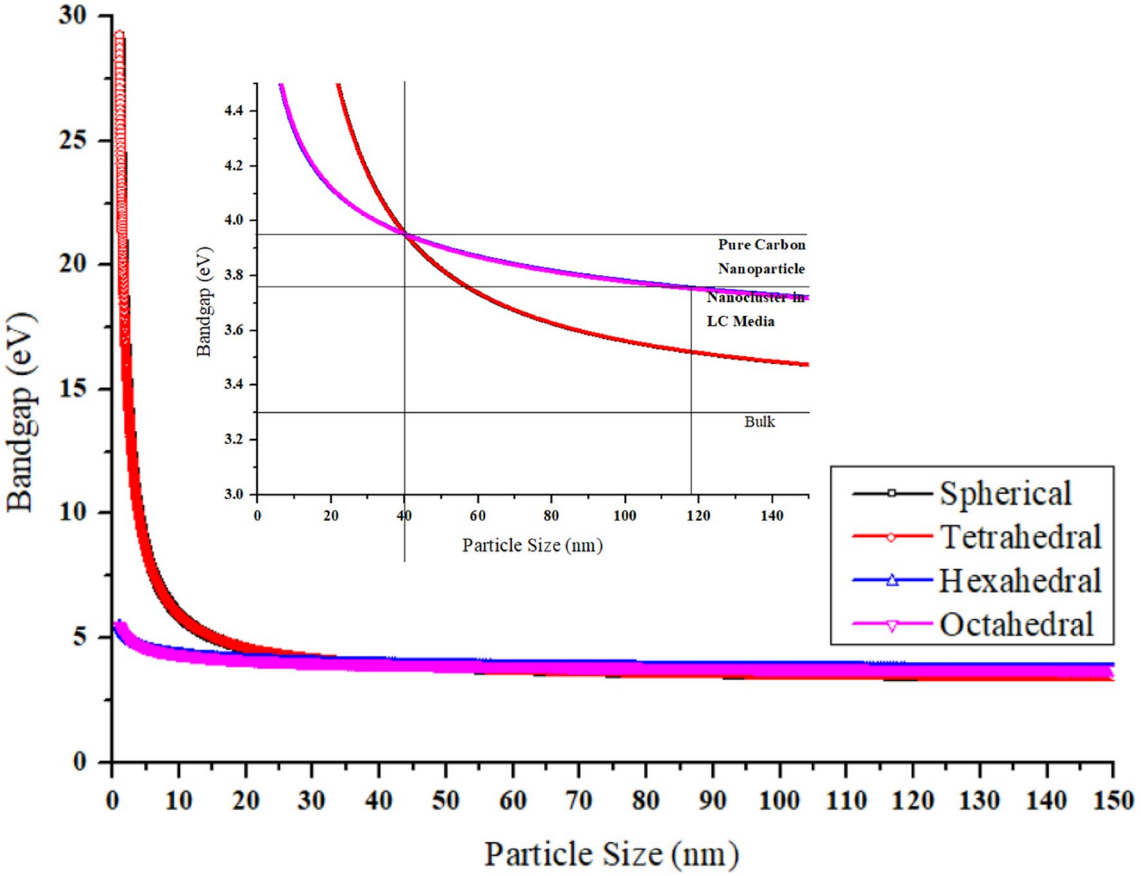


**Fig. 7** Variation of bandgap with size of nanoclusters

formed in presence of LC media and ethanol. We have plotted the Eq. (2) using these data and have solved for different shapes by extra-plotting the curve at different bandgaps. We observe that the best fit is obtained for the case of hexahedral shape. Using the carbon nanocluster doped LC system bandgap value, we have estimated the size of as 118 nm as shown in Fig. 7. This is simply a model-based estimation and the actual sizes may slightly vary.

## NMR spectroscopy

The ECS 400 MHz (JEOL) NMR spectrometer is used to observe NMR spectra. NMR spectroscopy reveals the molecular structure of organic and inorganic compounds present inside nanomaterials. By analyzing the chemical shifts, coupling constants, and relaxation periods of atomic nuclei, we may determine the connectivity, spatial organization, and conformational properties of molecules. The study reveals information about nearby atoms, groups of atoms, or function groups attached to an atom. NMR spectroscopy does not provide a picture of a molecule, but rather provides detailed information about its presence. The values of corresponding chemical shifts are given by the position on the NMR plot where nuclei absorb incident radiation. For 1H-NMR, these two standards have chemical shifts of 0.0 and 7.26, respectively. Peaks in the 7.091 ppm to 7.221 ppm range are caused by aromatic H- nuclei at two benzene rings. The other peaks in the range -0.1 ppm to 2.5 ppm are due to the presence of H nuclei present on carbon chain. The NMR data of pure LC Fig. 8a shows the presence of primary alkyl group R-$CH_3$ confirmed by shielding at 0.8 ppm, 0.9 ppm, 1.0 ppm. After doping of carbon nanoclusters, the peaks show some shifting towards lower ppm value Fig. 8b. The doublet peak at -0.031 ppm and -0.039 ppm in pure LC, transforms to singlet with shifting to -0.045 ppm. After doping eight peaks due to benzene rings present in pure LC converges to five peaks in the range 7.087 ppm to 7.218 ppm Fig. 8b. After doping of carbon nanocluster to the system there is only slight shift observed for the carbon chained H atoms present in the LC molecules. The splitting can

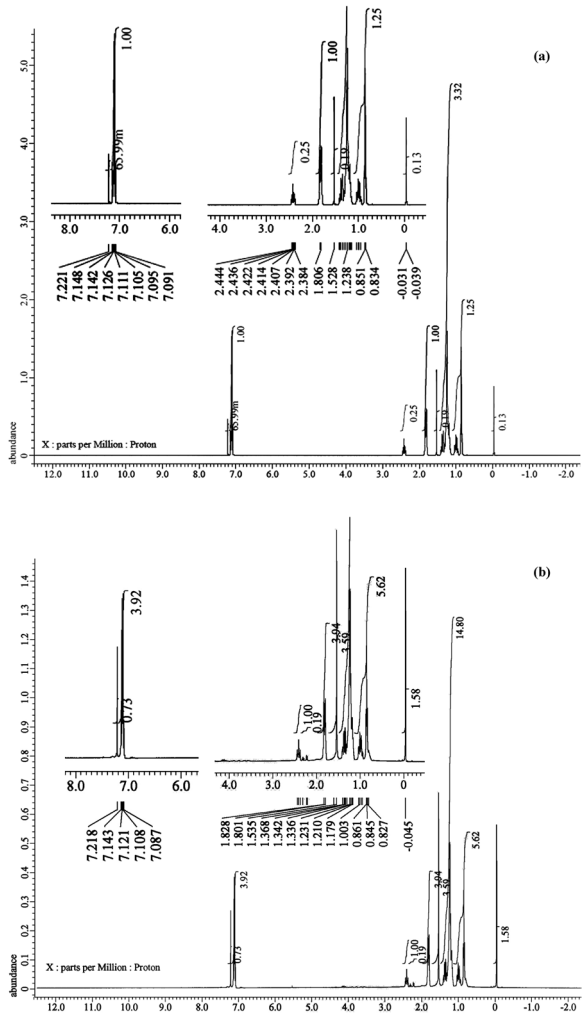


**Fig. 8** NMR spectra of **a** pure LC and **b** carbon nanocluster doped LC media

be clearly observed in enlarged peaks provided in insets of Fig. 8a, b.

## Conclusion

We have successfully synthesized nano-micro droplets using green synthesized carbon nanoclusters in LC media. Based on the interaction with surface molecules and dopant atoms, the shape of droplet formation in LC media alters. Due to the presence of $\pi$ -bond in graphene sheet it affects the atom agglomeration of carbon atom in LC media. The overlapping of orbitals confirms the strong interaction between the carbon cluster and graphene surface, due to this the carbon droplets are flattened on the graphene surface. The combination of different measurement techniques fulfilled two purposes. On the one hand, we aimed to learn about the creation of carbon nanoparticles and explore its properties as well as that of carbon-based nano-micro droplets. On the other hand, we have studied role of ITO and graphene surfaces on the formation of hierarchical structures. This research will aid in the design and development of new carbon nanomaterials with novel functions and improved performance, especially in presence of graphene. The findings also provide a useful guideline for device design in order to generate surface nanodroplets of various sizes. As a result of their widespread use in optoelectronic applications and their capacity to affect the behavior of carbon nanodot-based nano-micro droplets, ITO and graphene sheets were chosen as substrates for comparative study. We have gained molecular scale insights into the interaction between the nano-micro droplets and the substrate materials by examining these substrates. It may perhaps open the new pathways to design optoelectronic devices.

**Acknowledgements**
The authors are thankful to Dr. Jurgen Schnitker, Wavefunction Inc., California, USA, for providing us Spartan 20 Software. They are thankful to Dr. K Awasthi, MRC, MNIT, Jaipur, Dr Prabhat K Dwivedi, Senior Scientific Officer, Nanoscience Center, IIT Kanpur and Prof. R. K. Tiwari, DDU Gorakhpur University, Uttar Pradesh, India for extending their support.

**Author contributions**
All authors have contributed as per the credit given.

**Funding**
No funding has been received to carry out this research work.

**Availability of data and materials**
Data and material will be made available on request.

## Declarations

**Consent for publication**
All authors have read the manuscript and agree for its publication.

**Competing interests**
Authors declare that they have no competing interests.

Received: 4 July 2023 Accepted: 27 October 2023
Published online: 30 November 2023

**References**

1. Chen X, Bagnall D, Nasiri N (2023) Capillary-driven self-assembled microclusters for highly performing UV photodetectors. Adv Funct Mater 2302808:1–10
2. Singh AK, Singh SP (2022) Revisiting hierarchical arrangement of quantum dots in presence of liquid crystal media. Mol Cryst Liq Cryst 46:1–47
3. Qu R, Li G (2022) Overview of liquid crystal biosensors: from basic theory to advanced applications. Biosensors. https://doi.org/10.3390/bios12040205
4. Shen Y, Dierking I (2019) Perspectives in liquid-crystal-aided nanotechnology and nanoscience. Appl Sci 9:2512
5. Ouskova E, Buluy O, Blanc C et al (2010) Enhanced magneto-optical properties of suspensions of spindle type mono-dispersed hematite nano-particles in liquid crystal. Mol Cryst Liq Cryst 525:104–111

6. Zaytseva O, Neumann G (2016) Carbon nanomaterials : production, impact on plant development, agricultural and environmental applications. Chem Biol Technol Agric 3:1–26
7. Kah M, Hofmann T (2015) The challenge: carbon nanomaterials in the environment: newthreats or wonder materials? Environ Toxicol Chem 34:1–5. https://doi.org/10.1002/etc.2898
8. Cui L, Ren X, Sun M, Liu H, Xia L (2021) Carbon dots: synthesis, properties and applications. Nanomaterials 11(12):3419
9. Scaria J, Karim AV, Divyapriya G et al (2020) Carbon-supported semiconductor nanoparticles as effective photocatalysts for water and wastewater treatment. Nano-Mater Photocatal Degrad Environ Pollut. https://doi.org/10.1016/B978-0-12-818598-8.00013-4
10. Georgakilas V, Perman JA, Tucek J et al (2015) Broad family of carbon nanoallotropes : classi fi cation, chemistry, and applications of fullerenes, carbon dots, nanotubes, graphene, nanodiamonds, and combined superstructures. Chem Rev. https://doi.org/10.1021/cr500304f
11. Tiwari SK, Sahoo S, Huczko A (2020) Graphene research and their outputs: status and prospect. J Sci Adv Mater Dev. https://doi.org/10.1016/j.jsamd.2020.01.006
12. Avouris P, Dimitrakopoulos C (2012) Graphene: synthesis and Graphene, since the demonstration of its easy isolation by the exfoliation of. Mater Today 15:86–97. https://doi.org/10.1016/S1369-7021(12)70044-5
13. Grajek H, Jonik J, Witkiewicz Z et al (2019) Critical reviews in analytical chemistry applications of graphene and its derivatives in chemical analysis applications of graphene and its derivatives in chemical analysis. Crit Rev Anal Chem 50:1–27. https://doi.org/10.1080/10408347.2019.1653165
14. Kusmartsev FV, Wu WM, Pierpoint MP et al (2014) Application of graphene within optoelectronic devices and transistors. Springer, Singapore
15. Miinz W, Smith IJ, Lewis DB et al (1997) Droplet formation on steel substrates during cathodic steered arc metal ion etching. Vacuum 48:473–481
16. Zhang X, Lu Z, Tan H et al (2015) Formation of surface nanodroplets under controlled flow conditions. Proc Natl Acad Sci 112:9253–9257
17. Qian J, Arends GF, Zhang X (2019) Surface nanodroplets formation dissolution and applications. Langmuir. https://doi.org/10.1021/acs.langmuir.9b01051
18. He B, Yang S, Qin Z et al (2017) The roles of wettability and surface tension in droplet formation during inkjet printing. Sci Rep. https://doi.org/10.1038/s41598-017-12189-7
19. Theberge AB, Courtois F, Schaerli Y, et al (2010) Reactions in Microdroplets Microdroplets in Microfluidics : An Evolving Platform for Discoveries in Chemistry and Biology Angewandte. 5846–5868
20. Khandekar S, Kumar S, Muralidhar K (2012) Dropwise condensation studies on multiple scales dropwise condensation studies on multiple scales. Heat Transfer Eng. https://doi.org/10.1080/01457632.2012.611463
21. Sohrabi S, Moraveji MK (2020) Droplet microfluidics: fundamentals and its advanced applications. RSC Adv 10(46):27560–27574. https://doi.org/10.1039/d0ra04566g
22. Salimi H, Bushra R, Shakeel N et al (2023) Papaya peel waste carbon dots / reduced graphene oxide nanocomposite: from photocatalytic decomposition of methylene blue to antimicrobial activity. J Bioresour Bioprod. https://doi.org/10.1016/j.jobab.2023.01.009
23. Eskalen H (2020) Influence of carbon quantum dots on electro—optical performance of nematic liquid crystal. Appl Phys A 126:1–10. https://doi.org/10.1007/s00339-020-03906-7
24. Yaglioglu HG, Balci S (2022) Strong coupling of carbon quantum dots in liquid crystals. J Phys Chem Lett. https://doi.org/10.1021/acs.jpclett.1c03937
25. Rastogi A, Hegde G, Manohar R (2020) Effect of oil palm leaf-based carbon quantum dot on nematic liquid crystal and its electro-optical effects. Liquid Crystals. https://doi.org/10.1080/02678292.2020.1817997
26. Mazzier D, Favaro M, Agnoli S, Silvestrini S, Granozzi G, Maggini M, Moretto A (2012) Synthesis of luminescent 3D microstructures formed by carbon quantum dots and their self-assembly properties. Chem Comm. https://doi.org/10.1039/C4CC02496F
27. Zhan J, Lei Z, Zhang Y (2022) Review non-covalent interactions of graphene surface : mechanisms and applications. CHEMPR. 8:947–979. https://doi.org/10.1016/j.chempr.2021.12.015
28. Son S, An J, Choi J et al (2021) Surface-anchored alkylated graphene oxide as a two-dimensional homeotropic alignment layer for nematic liquid crystals. Mater Today Commun 28:102539. https://doi.org/10.1016/j.mtcomm.2021.102539
29. Meng X, Chen T, Li Y et al (2019) Assembly of carbon nanodots in graphene-based composite for flexible electro-thermal heater with ultrahigh efficiency. Nano Res 12:1–11
30. Chai Z, Childress A, Busnaina AA (2022) Directed assembly of nanomaterials formaking nanoscale devices and structures: mechanisms and applications. ACS Nano 16:17641–17686
31. Moreno G, Alessandro A, Luisa A. (2021) Aggregation - Induced Emission in Electrochemiluminescence : Advances and Perspectives. 65–90
32. Singh AK, Singh SP (2023) Formation of nano and micro scale hierarchical structures in MgO and ZnO quantum dots doped LC media: the role of competitive forces. Condens Matter Phys 26:4
33. Singh AK, Singh SP (2023) Molecular scale insights from NMR studies of hybrid systems formed via doping silver QDs in 6CHBT liquid crystal: a quantitative investigation of their optoelectronic properties. Liq Cryst. https://doi.org/10.1080/02678292.2023.2227979
34. Abd AH, Ibrahim OA (2022) Synthesis of carbon quantum dot by electrochemical method and studying optical. Electrical, and Structural Properties 6:823–830
35. Tune D, Tune DD, Flavel BS et al (2010) Single walled carbon nanotube network electrodes for dye solar cells solar energy materials & solar cells single walled carbon nanotube network electrodes for dye solar cells. Sol Energy Mater Sol Cells 94:1665–1672. https://doi.org/10.1016/j.solmat.2010.05.026
36. Singh AK, Singh SP (2022) Band-gap-tailoring in liquid crystals: organizing metal atoms and nanoclusters in LC media. Liq Cryst 49:605–632
37. Jena L, Soren D, Deheri PK et al (2021) Current research in green and sustainable chemistry preparation, characterization and optical properties evaluations of bamboo charcoal. Curr Res Green Sustain Chem 4:100077. https://doi.org/10.1016/j.crgsc.2021.100077


## Publisher's Note